Marine Pollution Bulletin 216 (2025) 117982

Contents lists available at ScienceDirect

Marine Pollution Bulletin

journal homepage: www.elsevier.com/locate/marpolbul

Biogeochemical and microbial community responses to anthropogenic nutrient inputs into the Solent

Lukas Marx [a,*], Michelle Hale [a], B.B. Cael [b], Sarah Reynolds [a]

[a] School of the Environment, Geology and Geosciences, University of Portsmouth, Portsmouth, United Kingdom
[b] Ocean BioGeosciences, National Oceanography Centre, Southampton, United Kingdom

ARTICLE INFO

Keywords:
Coastal ocean
Biogeochemical cycling
Primary production
Nutrient pollution
Climate change
Anthropogenic pressure

ABSTRACT

Given their pivotal role in providing essential ecosystem services, understanding the dynamics of coastal waters and their responses to disturbances such as climate change and nutrient pollution is imperative. In this study, we conducted year-long monitoring (May 2021 to May 2022) of the pico- and nanoplanktonic community driving biogeochemical cycling in waters of the Solent on the south coast of the UK. Our investigation revealed that the Solent receives excess nutrient influxes year-round, attributable to sewage spills transported through the intertidal Langstone Harbour, amounting 45.4 ± 14.8 t NO_3^- and 2.5 ± 0.5 t PO_4^{3-} per year. However, these, and sub-annual environmental fluctuations appear not to impede phytoplanktonic succession and associated ecosystem functioning, with observed planktonic blooms in spring (2.46–5.96 μg L^{-1} chlorophyll *a*) and late summer (3.85 μg L^{-1} chlorophyll *a*), despite a warming event in July 2021. These results underscore the importance of continuous monitoring of point sources of nutrient pollution to discern long-term trends and interannual variability of ecosystem functioning in the Solent.

1. Introduction

Coastal settings and transitional waters are invaluable and highly productive ecosystems, accounting for −0.20 ± 0.02 Pg carbon (C) yr^{-1} of carbon sink activity, a flux density comparable to the open ocean (Roobaert et al., 2019; Hauck et al., 2020). Acting as boundary systems between fresh and marine waters, the coastal ocean provides important ecosystem services, including forming the base of the marine food web, acting as nursery grounds and as important locations for migratory species, both aquatic and terrestrial. Temperate coastal environments are under ever increasing threats from urban development and climate change, namely rising sea level and temperature, more frequently occurring extreme meteorological events, and increasing ocean acidification (OA) (Pontee, 2013; IPCC, 2021; Gac et al., 2021). Shallow water and tidal regimes make coastal water bodies particularly prone to the intensified effects of climate change and anthropogenic pressures such as nutrient pollution from urban and agricultural runoff and wastewater discharge, whereby increased nutrient loading alters the natural state drastically, causing more frequently occurring eutrophication and harmful algal blooms (Moore et al., 2013; Naden et al., 2016; Devlin et al., 2023). Although legislations have been put in place to limit anthropogenic nutrient inputs into coastal waters, many regions are still affected by eutrophic conditions, with the most notable being the Baltic Sea and the Gulf of Mexico (Boyes and Elliott, 2006). The effects of eutrophic waters on the health of the marine coastal ecosystem include increased algal growth and inducing shading of the lower water column and benthic system by increasing turbidity and decreasing oxygen concentrations. Such impacts influence the ability of the ecosystem to function successfully and ultimately lower ecosystem productivity. It is therefore imperative to monitor coastal systems to observe annual and inter-annual variability and the long-term impacts of climate change and anthropogenically induced stressors, both on the environmental setting and the planktonic community (Harris, 2010). More recently, monitoring of pico- and nanoplankton groups has emerged as an important ecosystem health indicator. This size class (< 20 μm) can reach up to three orders of magnitude higher abundances than larger planktonic groups, thus account for a major portion of the pelagic biomass and perturbations in abundance or community structure can be linked to changes in environmental pressures or nutrient loading (McQuatters-Gollop et al., 2024).

The Solent, an estuarine straight in the English Channel, is experiencing some of the fastest rates of warming around the UK, with

* Corresponding author presently at: Department of Chemistry and Geochemistry, Woods Hole Oceanographic Institution, Woods Hole, MA, United States.
E-mail addresses: lukas.marx@whoi.edu (L. Marx), michelle.hale@port.ac.uk (M. Hale), cael@noc.ac.uk (B.B. Cael), sarah.reynolds@port.ac.uk (S. Reynolds).

https://doi.org/10.1016/j.marpolbul.2025.117982
Received 8 July 2024; Received in revised form 12 March 2025; Accepted 11 April 2025
Available online 16 April 2025

temperature increases of 0.42 °C per decade (Kassem et al., 2023). In combination with anthropogenic emissions, the region has been increasingly acidifying, with the pH decreasing by 0.0046 yr^{-1} between 2008 and 2020, largely due to atmospheric CO_2 forcing (57–66 %) and increased sea surface temperature (31–37 %) (Gac et al., 2021). Additionally, by 2010, 97 kt nitrogen (N) yr^{-1} and 14.8 kt phosphorus (P) yr^{-1} from sewage discharges have increased the nutrient loading throughout water bodies in the UK, most of which reaches the coastal ocean (Naden et al., 2016; Bell et al., 2021). Although the EU Urban Waste Water Treatment Directive (UWWTD, 91/271/EEC) was adopted into UK legislation in 1994 (and its post-BREXIT equivalent), and resulted in a decrease of 67 % of phosphorus and 97 % of ammonia loading since then, total nitrogen (with 90 % being nitrate-N) in UK waters, however, has increased by 29 % since 1970 (Boyes and Elliott, 2006; Tappin and Millward, 2015; Naden et al., 2016; Liu et al., 2021; Environmental Audit Committee, 2022). As a result, increased algal biomass, indicative of eutrophication, have been observed in coastal locations throughout the Solent in the English Channel, such as Portsmouth, Chichester and Langstone Harbour (Tappin and Millward, 2015, Painting et al., 2016. Devlin et al., 2023).

The semi-enclosed Langstone Harbour is an area of national and international significance from an ecological perspective and is highly

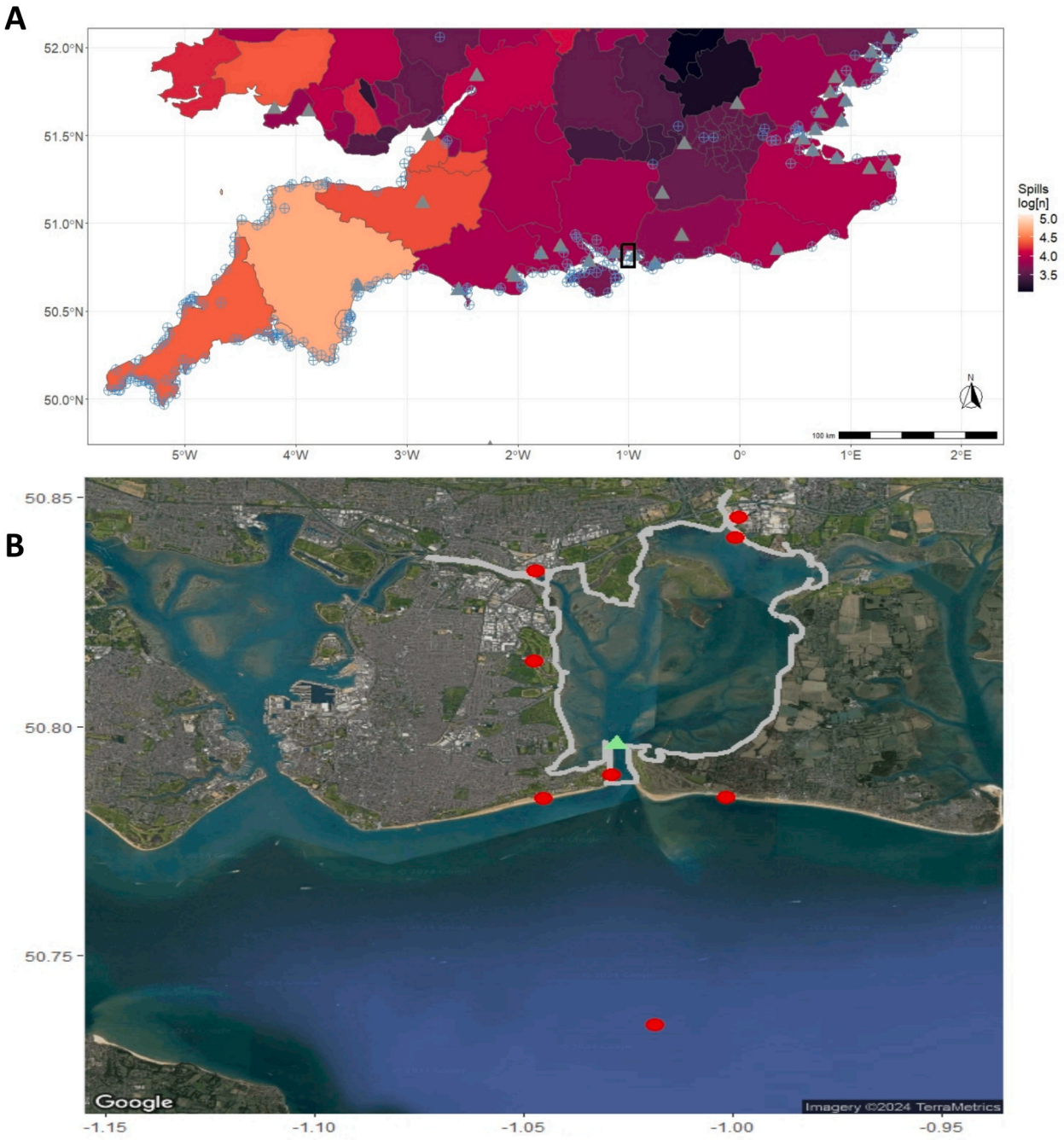

Fig. 1. **A** Map of South UK with designated RAMSAR sites (grey pyramids) and marine Sites of Special Scientific Interest (SSSI, light blue circles). Colour shading shows stormwater and sewage overflow events (in log[n]) per county for 2021 and 2022. Black rectangle shows the location of Langstone Harbour. **B** Satellite imagery of study site with grey shapefile showing the extent of Langstone Harbour, green pyramid the monitoring station and red dots indicating point sources of stormwater and sewage releases. (For interpretation of the references to colour in this figure legend, the reader is referred to the web version of this article.)

protected by EU and UK directives; a RAMSAR designated wetland of international importance (https://www.ramsar.org/), a Special Protection Area (SPA), Special Area of Conservation (SAC), a Site of Special Scientific Interest (SSSI), an Area of Outstanding Natural Beauty (AONB), and a Royal Society for the Protection of Birds Nature Reserve (RSBP). Despite its high conservation status and increased effort to conserve saltmarshes and seagrass meadows, and restore natural oyster populations (Foster et al., 2013; Helmer et al., 2019; Watson et al., 2020), long-term data series of environmental and biological conditions in the harbour are lacking. Labelled a potential problem area for eutrophication (Painting et al., 2016), it is becoming inherently more important to monitor Langstone Harbour and its drainage into the Solent. Specifically, a wastewater treatment facility serving >400,000 households acts as a point source of treated effluent, but also untreated stormwater and wastewater releases into the Solent. Therefore, we conducted a year-long monitoring of environmental conditions, dissolved and particulate nutrient pools (nitrogen = N, phosphorus = P) and pico- and nanoplanktonic community structure at the outflow of Langstone Harbour into the Solent between May 2021 and May 2022. The insights gained from this monitoring will help to improve the understanding of the response of such coastal waters to anthropogenic nutrient inputs.

2. Material and methods

2.1. Site description

Langstone Harbour is a semi-enclosed intertidal bay with water depths ranging between 0.5 and 5.3 m on the south coast of the UK (50.8167°N, 1.0000°W) (Fig. 1). Although Langstone Harbour is connected with Portsmouth Harbour and Chichester Harbour via small freshwater channels, it can be assumed a single point source into the Solent, due to a near complete drainage at low tides. The local wastewater treatment facility is located at the head of Langstone Harbour and its effluents are transported through the bay into the Solent during low tide. The macrotidal Solent experiences a strong semi-diurnal regime with a double high water tidal cycle, a typical land-seaward current of 0.02–0.03 m s^{-1}, a seaward-land current of 0.01–0.02 m s^{-1}, and a general seaward flow in the eastern Solent, leading to water exchange within the straight of 20–25 % per tidal cycle (Levasseur, 2008). The monitoring station was set up on May 6, 2021, at the drainage of Langstone Harbour into the Solent, approximately 15 m from shoreline, where water depth is consistently above 5 m. Here, on a weekly basis, 5 L of natural seawater was collected into a shaded carboy and transported to the Institute of Marine Sciences (IMS) for subsampling, whilst environmental conditions (temperature, salinity, pH and dissolved oxygen (DO)) were recorded in 15 min intervals by an EXO2 multiparameter sonde (YSI).

2.2. Sampling and analytical procedures

Dissolved inorganic nutrients were collected into 60 mL HDPE bottle by filtration over acid-washed and combusted (450 °C, 4 h) GF/F filters (Whatman GF/F, 25 mm, 0.7 μm pore size). Samples were stored frozen at −20 °C until analysis on a 4-channel autoanalyser AA500 (SEAL analytical). Nitrate (NO_3^-), nitrite (NO_2^-), dissolved silicate (DSi) and phosphate (PO_4^{3-}) were analysed against certified reference materials (KANSO) and repeated measurements of these yielded long-term standard deviations of 0.027 μM, 0.004 μM, 0.023 μM and 0.004 μM, respectively.

Samples for dissolved organic phosphorus (DOP) were collected and stored in the same manner and analysed as soluble reactive phosphorus (SRP) via high temperature oxidation with potassium persulfate and MAGIC precipitation (following Lomas et al., 2010 and Davis et al., 2014, 2019) on the AA500 with a long-term standard deviation of 0.004 μM. DOP was ultimately determined as the difference between SRP and PO_4^{3-}.

Samples for particulate organic carbon (POC) and nitrogen (PON) were collected as organic matter retained after filtration of 250 mL through acid-washed and pre-combusted GF/F filters and stored frozen at −20 °C until analysis. Filters were dried at 40 °C and following vapour phase decarbonisation (following Yamamuro and Kayanne, 1995), analysed on a Flash2000 elemental analyser against standard reference material Nicotinamide (Thermo Scientific). Accuracy of analyses was within 5 % of standard values with a precision of ±0.28 μg L^{-1} for POC and ± 0.36 μg L^{-1} for PON.

Samples for particulate phosphorus (PP) were also collected after filtration of 250 mL through GF/F filters and analysed following Davis et al. (2014) after high-temperature combustion (500 °C for 4 h) and acid extraction as dissolved phosphorus on the AA500. The accuracy of the analysis had a relative standard deviation of 2.42 % with a related uncertainty of 0.03 μM. All measurements for PP were converted to μg L^{-1}.

The determination and enumeration of the pico- and nanoplanktonic community (particle sizes between 0.1 and 20 μm) was conducted with flow cytometry: 4 mL of unfiltered sample water were fixed with 40 μl 50 % Glutaraldehyde solution to reach a final concentration of 0.5 % and then stored at −80 °C until analysis on a CyFlow Cube 8 flow cytometer (Sysmex) following Tarran and Bruun (2015). The results were validated by congruent analysis of flow-set polystyrene fluorosphere beads (diameter 3.6 μm, Beckman Coulter).

Chlorophyll *a* (Chl *a*) and pheophytin *a* were determined according to the Joint Global Ocean Flux Study (JGOFS) acidification method (Knap et al., 1996). Briefly, organic material was collected by filtration of 100 mL sample water on GF/F filters and pigments subsequently extracted in 90 % Acetone at −20 °C overnight. The extract was homogenized and analysed on a Trilogy benchtop fluorometer (Turner Designs) before and after acidification with 0.1 N HCl. Accuracy of analyses was monitored with solid standards and was within 5 %.

2.3. Statistical analysis

Statistical analyses were conducted in RStudio version 1.4.1106 (R Core Team, 2022) on the condensed monthly averages of the dataset to identify seasonal variability by correlating the parameters measured and evaluating their associations. As such, a Shapiro-Wilk multivariate normality test was performed and revealed a non-normal distributed dataset ($p < 0.001$)) (Shapiro and Wilk, 1965). Accordingly, Spearman ρ correlations were applied, whilst non-parametric Kruskal-Wallis tests were used to determine significance of environmental parameters between seasons (Kruskal and Wallis, 1952). To evaluate the input of excess nutrients from sewage and stormwater outfalls, we first calculated a rolling seasonal mean of nutrient concentrations and correlated it with the reported spill incidents (made publicly available by the wastewater operator under https://www.southernwater.co.uk/about-us/environmental-performance/healthy-rivers-and-seas/flow-and-spill-reporting/) (Supplementary data). We then performed a linear regression on the subset of the data where spill incidents were reported, with setting the intercept to 0, whereby the slope represents the excess nutrients per spill duration.

3. Results

3.1. Environmental conditions at monitoring station

The environmental conditions at our monitoring site showed clear seasonal differences (Table 1). Water temperatures were highest in summer and surpassed 20 °C in June and July 2021, then decreased during autumn to lowest temperatures measured in winter (8.5–9.2 °C). The elevated temperature in June and July 2021 suggested the occurrence of a temporary warming event. Congruent with temperature dynamics, dissolved oxygen (DO) in the water column was lowest in

Table 1
Environmental conditions as averages (+SD) per month between May 2021 and May 2022: Measured mean temperature (°C), salinity (psu), pH and dissolved oxygen (DO, mg L^{-1}) from EXO2 multiparameter sonde.

	Temperature	*Salinity*	*pH*	*DO*
	[°C]	*[psu]*		*[mg L^{-1}]*
May 21	12.9 ± 1.1	33.7 ± 0.1	8.3 ± 0.04	8.5 ± 0.2
Jun 21	17.4 ± 1.2	34.0 ± 0.1	8.2 ± 0.02	7.6 ± 0.3
Jul 21	20.2 ± 1.7	33.9 ± 0.2	8.2 ± 0.05	7.1 ± 0.6
Aug 21	20.2 ± 1.2	34.0 ± 0.6	8.2 ± 0.12	6.7 ± 1.1
Sep 21	18.7 ± 1.2	33.8 ± 0.1	8.2 ± 0.03	7.3 ± 0.3
Oct21	16.0 ± 0.6	33.0 ± 0.4	8.2 ± 0.03	7.4 ± 0.5
Nov21	12.6 ± 1.5	33.0 ± 0.4	8.3 ± 0.03	8.3 ± 0.3
Dec21	8.9 ± 0.1	33.1 ± 0.1	8.3 ± 0.01	9.1 ± 0.1
Jan22	8.5 ± 0.7	33.3 ± 0.2	8.4 ± 0.02	9.2 ± 0.2
Feb22	9.2 ± 0.4	32.8 ± 0.7	8.4 ± 0.01	9.9 ± 0.3
Mar22	10.2 ± 1.4	33.2 ± 0.3	8.4 ± 0.14	8.5 ± 1.5
Apr22	12.0 ± 0.9	33.1 ± 0.2	8.6 ± 0.03	8.9 ± 0.1
May 22	15.5 ± 0.9	33.8 ± 0.1	8.6 ± 0.01	8.1 ± 0.3

summer (< 8 mg L^{-1}) and highest (> 9 mg L^{-1}) in winter. pH remained rather uniform (8.2–8.3) throughout the year-long observation, but did increase during spring 2022 (to 8.6). Salinity at the monitoring site ranged between 33 and 34 psu throughout, thus clearly indicating a fully marine rather than a transitional water body.

3.2. Nutrient dynamics at monitoring station

Nutrient dynamics indicated a clear seasonality, with maximum concentrations measured in January and February 2021, and lowest concentrations measured in April and June 2021 (Fig. 2). Generally, nutrient concentrations in winter were significantly higher than in summer (Kruskal-Wallis χ^2 (2), $p < 0.001$ for NO_3^- and PO_4^{3-} and χ^2 (2), $p < 0.05$ for NO_2^- and DSi). A substantial reduction in nutrients (−66 ± 3 %) occurred during spring, with an increase in concentrations observed between September and October (67 ± 17 %). The mean concentrations (± SD) measured for NO_3^- (0.9 ± 0.6 µmol L^{-1}) and PO_4^{3-} (0.09 ± 0.03 µmol L^{-1}) were lowest in summer, whilst NO_2^- (0.07 ± 0.05 µmol L^{-1}) and DSi (3.6 ± 2.5 µmol L^{-1}) were lowest in spring. The reduction of nutrients during spring led to a nutrient-exhausted system over summer, whereas the nutrient loading at the monitoring station increased substantially in autumn (NO_3^- 6.8 ± 5.3 µmol L^{-1}, NO_2^- 0.22 ± 0.14 µmol L^{-1}, DSi 6.3 ± 2.1 µmol L^{-1} and PO_4^{3-} 0.35 ± 0.16 µmol L^{-1}), reaching highest concentrations in winter (19.1 ± 5.1, 0.24 ± 0.08, 9.4 ± 1.4 and 0.51 ± 0.04 µmol L^{-1}, respectively). Following these sub-annual nutrient dynamics, the inorganic N:P ratio often greatly deviated from the canonical Redfield ratio of 16:1 (Fig. 3). Due to the near complete depletion of N sources and PO_4^{3-} in summer, the water column exhibited the N:P ratio of 10 ± 3, significantly lower than a ratio of 38 ± 8 in winter (Kruskal-Wallis χ^2 (2), $p < 0.001$), where the highest concentrations of NO_3^-, NO_2^- and PO_4^{3-} were measured. A N:P ratio of 35 ± 23 in spring revealed high fluctuations in nutrient utilisation, similar to autumn (17 ± 9), during which the N:P ratio was closer to Redfield.

3.3. Pigment dynamics at monitoring site

Lowest mean concentrations of Chl *a* were measured in winter (0.94 ± 0.22 µg L^{-1}), whilst significantly higher concentrations, with a mean of 2.11 ± 0.31 µg L^{-1}, were observed in spring (Kruskal-Wallis χ^2 (2), $p < 0.01$) (Fig. 3). Chl *a* concentrations in summer and autumn were intermediate at 1.43 ± 0.72 and 1.11 ± 0.27 µg L^{-1}, respectively. Peaks in Chl *a* were observed in August 2021 (3.85 µg L^{-1}), March 2022 (2.46–5.96 µg L^{-1}) and in May 2022 (3.7 µg L^{-1}), suggesting the occurrence of planktonic blooming episodes. The degradation product of Chl *a*, pheophytin *a* (an indication of phytoplankton mortality), was measured at highest concentrations in summer (1.88 ± 1.46 µg L^{-1}) and lowest in autumn (0.79 ± 0.24 µg L^{-1}) (Fig. 3). In both spring and

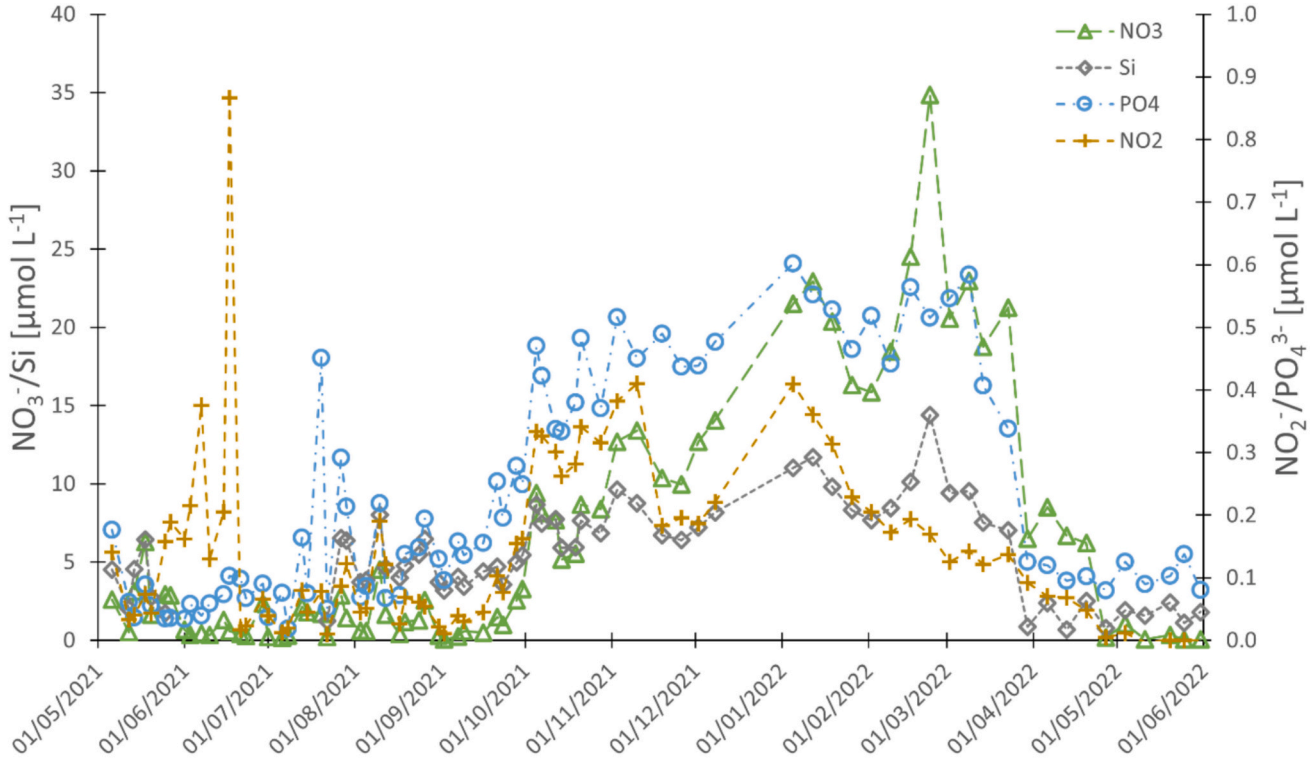

Fig. 2. Measured concentrations (µmol L^{-1}) of NO_3^- (green pyramids), NO_2^- (orange crosses), DSi (grey diamonds) and PO_4^{3-} (blue circles) at the monitoring station. Data points collected weekly between 06/05/2021–30/05/2022. (For interpretation of the references to colour in this figure legend, the reader is referred to the web version of this article.)

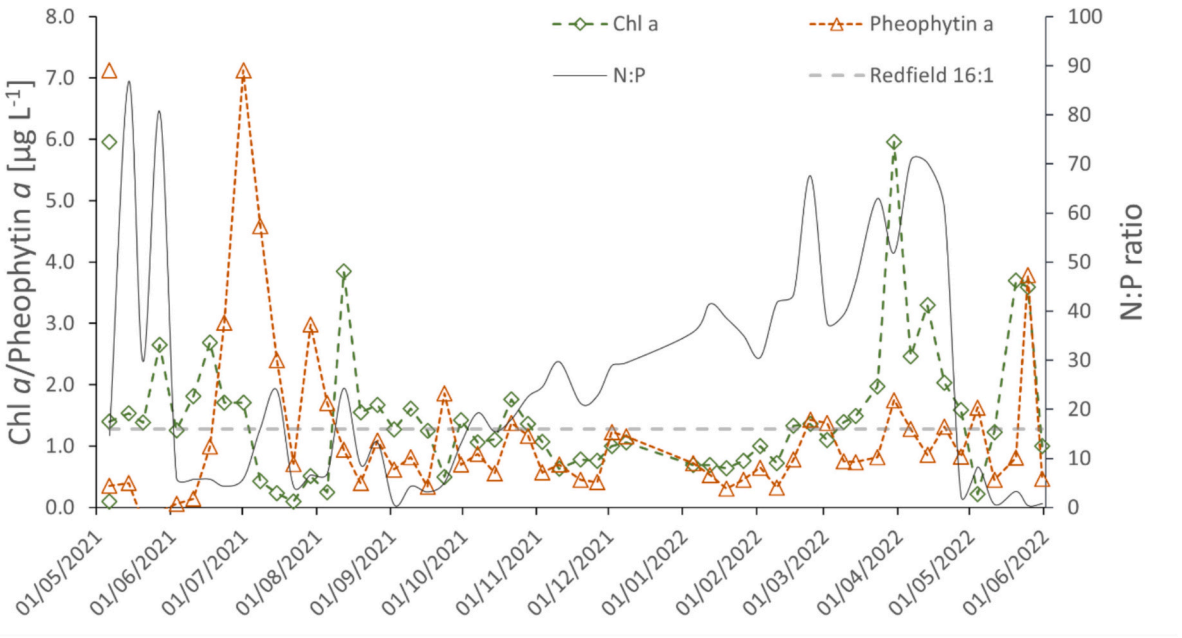

Fig. 3. Measured concentrations (µg L^{-1}) of chlorophyll *a* (green diamonds) and pheophytin a (orange pyramids) at the monitoring station from weekly sampling between 06/05/2021–30/05/2022. Grey dotted line depicts Redfield N:P ratio of 16:1 and solid line displays the N:P ratio of measured dissolved inorganic nutrient concentrations. (For interpretation of the references to colour in this figure legend, the reader is referred to the web version of this article.)

winter, pheophytin *a* was measured at intermediate levels (0.99 ± 0.44 and 0.83 ± 0.34 µg L^{-1}, respectively). As with Chl *a*, peaks of pheophytin *a* were observed. In July 2021 pheophytin *a* was measured at 7.13 µg L^{-1} and was elevated throughout this month relative to the rest of the year, suggesting enhanced phytoplanktonic mortality due to the breakdown of the spring bloom and potential impacts of the observed warming event. A second peak in pheophytin *a* (3.79 µg L^{-1}) was measured in May 2022 during the breakdown of the blooming event.

3.4. Microbial community structure at monitoring site

The determination of the pico- and nanoplanktonic community structure revealed five main phytoplanktonic groups: cyanobacteria (*Synechococcus*), cryptophyte algae, two size classes (pico- and nano-) of eukaryotes and coccolithophore species. A clear seasonal pattern was identified and aligned with the dynamics in pigments (Fig. 4A). Pico- and nanoplankton were most abundant in summer and cell counts decreased substantially in winter: mean abundance in winter was 4992 ± 1679 cell counts mL^{-1} and increased to 14,456 ± 3128 cell counts mL^{-1} in summer. Peak abundance was measured in July 2021 at 17712 cell counts mL^{-1}, whilst in January 2022 the community decreased to only 3391 cell counts mL^{-1}, equivalent to an 81 % decrease in total cell counts. The abundance planktonic cells in summer was significantly higher than in winter (Kruskal-Wallis χ^2 (2), $p < 0.001$). Both spring and autumn displayed intermediate abundance (6250 ± 1324 and 7461 ± 2379 cell counts mL^{-1}, respectively), closer to winter averages than the high abundances observed in summer. The pico- and nanoplanktonic community was consistently (with the only exception being May 2021) dominated by *Synechococcus*, which accounted for 70 ± 7 % of all cell counts (Fig. 4B). The second largest group were picoeukaryotes (20 ± 6 %), while the remaining three groups contributed jointly >10 ± 5 % (cryptophytes 3 ± 1 %, nanoeukaryotes 4 ± 2 % and coccolithophores 3 ± 2 %). The five groups further indicated differences across seasons with *Synechococcus* dominating the community structure throughout the year, the highest contribution to total cell counts was in winter (83 ± 2 %) and lowest in spring (57 ± 21 %). Conversely, all other groups had highest relative contributions in spring (cryptophytes 3 ± 1 %, picoeukaryotes 30 ± 21 %, nanoeukaryotes 6 ± 1 %, coccolithophores 4 ± 2 %). Moreover, cryptophytes, pico- and nanoeukaryotes contributed the least (2 ± 0.5 %, 9 ± 1 %, 4 ± 2 %, respectively) towards cell counts in winter. Coccolithophores were the exception and displayed the lowest counts in summer and contributed <1 % to the community structure.

3.5. Organic matter dynamics at monitoring site

Highest dissolved organic phosphorus (DOP) concentrations were measured in summer (0.24 ± 0.05 µmol L^{-1}), whilst concentrations during winter were below the detection limit (Table 2). Whilst the DOP pool in summer was apparently drawn down during autumn (0.01 ± 0.01 µmol L^{-1}), DOP increased over spring, although measurements showed high variability (0.12 ± 0.2 µmol L^{-1}). The dissolved P pool was dominated by the organic fraction in summer, with inorganic PO_4^{3-} being the main component in winter. Particulate organic matter (POM) also displayed seasonality in both concentrations and resulting stoichiometries (Table 2). Concentrations of particulate organic carbon (POC) and particulate phosphorus (PP) were highest in spring (259 ± 21 and 2.5 ± 0.2 µg L^{-1}, respectively), whilst particulate organic nitrogen (PON) was highest in autumn (74 ± 41 µg L^{-1}). Contrastingly, POC was lowest in autumn (171 ± 32 µg L^{-1}) and remained at intermediate concentrations in summer and winter. Both PON and PP were lowest in summer (23 ± 11 and 1.6 ± 0.1 µg L^{-1}, respectively). Strikingly, PON was elevated both in autumn and spring, whereas summer and winter displayed low concentrations. The resulting stoichiometric ratios of the POM pool mirrored the dynamics in concentrations measured: C:N and C:P ratios were highest in summer (10 ± 4 and 123 ± 20, respectively), whereas N:P was highest in autumn (42 ± 20). Low PON loading in summer led to a diminished N:P ratio of 14 ± 7, suggesting N limitation occurring during summer. Elevated C:N and C:P ratios in summer coincide with enhanced primary production and the formation of POM by the planktonic community.

3.6. Statistical analysis

The correlation analyses further evidenced the seasonality in nutrient dynamics, their involvement in pigment and community structure dynamics and subsequent formation of POM. Evidently,

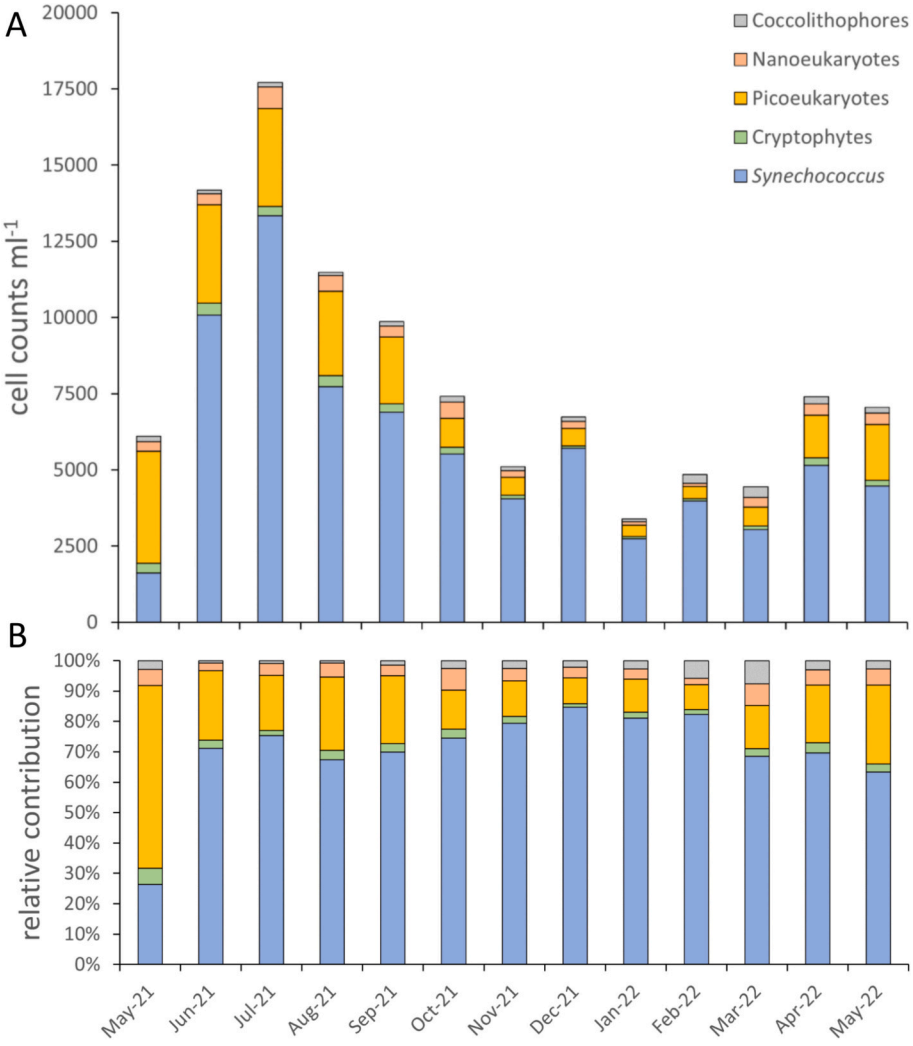

Fig. 4. Pico- and nanoplanktonic community structure: Synechococcus (blue), cryptophyte (green), picoeukaryotes (orange), nanoeukaryotes (red) and coccolithophores (grey). **A** shows abundance in cell counts mL^{-1}, **B** shows relative contribution towards the community. Data presented as monthly averages from May 2021 to May 2022. (For interpretation of the references to colour in this figure legend, the reader is referred to the web version of this article.)

Table 2
Seasonal organic matter dynamics at monitoring station: Concentrations of DOP (μmol L^{-1}), POC, PON and PP (μg L^{-1}) and stoichiometric ratios of the POM pool. Values and ratios are presented as seasonal means (± SD), with winter DOP measurements were below detection limit (BDL).

		Summer	*Autumn*	*Winter*	*Spring*
DOM	*DOP*	0.24 ± 0.05	0.01 ± 0.01	BDL	0.12 ± 0.2
POM	*POC*	202 ± 29	171 ± 32	202 ± 92	259 ± 21
	PON	23 ± 11	74 ± 41	46 ± 11	65 ± 13
	PP	1.6 ± 0.1	1.7 ± 0.3	2.3 ± 0.8	2.5 ± 0.2
	C:N	10 ± 4	4 ± 3	5 ± 3	4 ± 1
	N:P	14 ± 7	42 ± 20	23 ± 13	27 ± 7
	C:P	123 ± 20	105 ± 31	86 ± 22	105 ± 1

nutrient concentrations were higher in winter than in summer and thus negatively correlated with temperature (NO_2^- $r = -0.57$, $p = 0.044$; NO_3^- $r = -0.8$, $p = 0.001$; PO_4^{3-} $r = -0.63$, $p = 0.022$; DSi $r = -0.58$, $p = 0.039$). NO_3^- was the key driver for the N:P ratio of the inorganic pool ($r = 0.81$, $p = 0.001$) which also negatively correlated with temperature ($r = -0.74$, $p = 0.004$). Planktonic abundance appears to have been controlled by temperature, rather than nutrient availability. In particular, *Synechococcus*, the numerically dominant contributor to total planktonic abundance, was correlated with temperature ($r = 0.7$, $p = 0.073$), but did not correlate to Chl *a* ($r = -0.09$, $p = 0.762$). Chl *a* was however positively correlated with the eukaryotic groups and cryptophytes, suggesting that these organisms contributed relatively more to Chl *a* dynamics than *Synechococcus*. In contrast, *Synechococcus* abundance and temperature were both correlated with pheophytin *a* ($r = 0.57$, $p = 0.044$ and $r = 0.23$, $p = 0.459$, respectively). Similarly, nanoeukaryotes were also positively correlated with pheophytin *a* ($r = 0.52$, $p = 0.067$).

Increased phytoplankton abundance and biomass under higher temperatures also suggests enhanced organic matter production and evidently, DOP correlated strongly with temperature ($r = 0.71$, $p = 0.007$), with significant relationships also found with *Synechococcus* ($r = 0.39$, $p = 0.188$), cryptophytes ($r = 0.93$, $p \leq 0.001$), pico- ($r = 0.94$, $p \leq 0.001$) and nanoeukaryotes ($r = 0.66$, $p = 0.015$). Highest concentrations of POM were observed during periods of high production, i.e. blooming events in spring and autumn. Whilst no positive correlation of POC, PON and PP with the primary producers investigated here was found, algal and bacterial cells did show positive correlation, specifically with PON ($r = 0.52$, $p = 0.071$ and PON: $r = 0.53$, $p = 0.065$, for algae and heterotrophic bacteria respectively). A regression analysis with Chl *a* provided evidence of autochthonously produced POM (Fig. 5), suggesting that larger planktonic groups (> 20 μm), such as diatoms, might drive productivity. POC and PP yielded high regression coefficients with

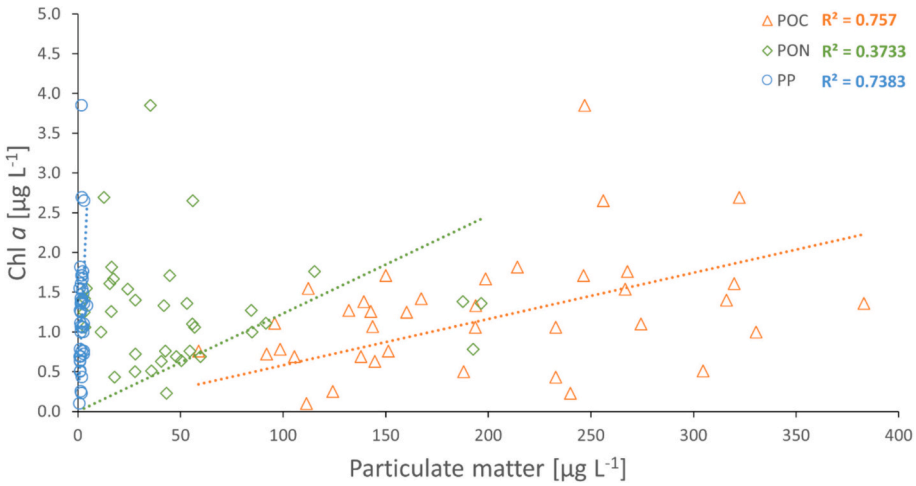

Fig. 5. Regression between chlorophyll *a* and particulate matter, including all sampling points between May 2021 and May 2022. POC (orange pyramids), PON (green diamonds) and PP (blue circles), dotted regression lines and respective R^2 values. (For interpretation of the references to colour in this figure legend, the reader is referred to the web version of this article.)

Chl *a* (R^2 = 0.76 and 0.74, respectively), whereas PON (R^2 = 0.37) indicated a substantial amount of fixed N originating from allochthonous sources outside of the system.

Analysis of storm- or wastewater overflow events reported for the Solent as the receiving water body revealed no correlation between PON and PP and spill duration ($r = 0.113$, $p = 0.475$ for PON and $r = 0.224$, $p = 0.153$ for PP). A correlation of spill duration and seasonal mean dissolved nutrient concentrations, however, showed substantial external nutrient inputs and caused nutrient anomalies for NO_3^- ($r = 0.519$, $p < 0.001$) and PO_4^{3-} ($r = 0.412$, $p < 0.01$). A linear regression between outfall duration and these anomalies revealed an excess nutrient input of 0.193 ± 0.061 µmol NO_3^- L^{-1} ($p < 0.01$) and 0.007 ± 0.002 µmol PO_4^{3-} L^{-1} ($p < 0.001$), over a spill duration of one hour.

4. Discussion

4.1. Assessing the threat on coastal settings from stormwater and sewage spills

Salinities measured (33–34 psu) clearly identify the monitoring location as marine rather than a transitional water body heavily influenced by freshwater inflow. Hence, we argument that our monitoring station indeed represents the Solent water body, rather than the intertidal Langstone Harbour. Due to near complete drainage of Langstone Harbour into the Solent, with water levels within the intertidal are lowering to 0.5 m during low tide, we conclude it to be a point source of nutrient pollution into the Solent. Further, due to the hydrological features in the eastern Solent and an sewage outflow pipe within the Solent estuarine Straight, complete flushing takes approximately 2 days or 4 full tidal cycles(Levasseur, 2008), hence nutrient pollution can persist at the monitoring station. Throughout the time of monitoring (May 2021 – May 2022), periodic elevations in dissolved inorganic nutrient loading occurred and could be attributed to 22 stormwater and sewage outfall incidents, amounting to a total of 500.76 h of spillage (Supplementary data). Around 85 % of the N-delivery by wastewater effluent into UK water bodies is associated with dissolved NO_3^- and indeed, NO_3^- levels at the monitoring station increased following such outfall incidents (Naden et al., 2016). Elevated nitrogen loading amounted to 0.193 ± 0.061 µmol excess N L^{-1} h^{-1} of spill duration. Likewise, PO_4^{3-} loading was elevated (0.007 ± 0.002 µmol excess P L^{-1} h^{-1} of spill duration) following outflow incidents, thus indicating that these discharges did not comply with the UWWTD Directive (Boyes and Elliott, 2006). Water companies in the UK are obligated to monitor the duration but not the volume of discharge, and discharges during exceptional rainfall are largely permitted. As such, an accurate evaluation of the amount of nutrient pollution remains largely enigmatic (Hammond et al., 2021). Here, based on flow rates presented in Hammond et al. (2021), scaled to a population size of 400,000, a first attempt of calculating an average amount of nutrient anomalies per year caused by the reported spill incidents was made. During the monitoring period (500.76 h of spill duration), the Solent received 30.3 ± 9.9 metric tons of NO_3^- and 2.7 ± 0.6 metric tons of PO_4^{3-}. For the whole year of 2021, 810.77 h of spills were recorded and 689.74 h for 2022, thus with an average of 750.25 h of spill duration per year, the Solent receives 45.4 ± 14.8 metric tons of NO_3^- yr^{-1} and 2.5 ± 0.5 metric tons of PO_4^{3-} yr^{-1} from sewage and stormwater outfalls. These estimates are lower than modelled estimates of 100–1000 t NO_3^- yr^{-1} and 10–100 t PO_4^{3-} yr^{-1} reported by Naden et al. (2016) and Bell et al. (2021). However, the estimates calculated here are likely much higher in reality, due to unreliable or non-apparent event duration monitoring by the operator, with reports made for only ~70 % of all stormwater and sewage overflows in 2020, which likely has not substantially increased since (Hammond et al., 2021). Although the excess amount of N and P delivered by stormwater and sewage spills are of comparably smaller magnitude than other influxes such as benthic pelagic nutrient coupling (Rühl et al., 2020), lateral transport by waves and tidal regime (Lønborg et al., 2021) or submarine groundwater discharge often exceeding riverine delivery (Santos et al., 2021). However, excess nutrients documented at the outflow of Langstone Harbour indicates a direct influence of such outfalls on water column nutrient loading in the Solent, which, given reasonable slow hydrological flushing might persist for several days (Levasseur, 2008). In fact, the N-loading measured surpassed winter mean threshold values (18 µmol L^{-1}) for coastal water bodies set by the EU Water Framework Directive (WFD; 2000/60/EC), implying a direct contribution of these outfalls to Langstone Harbour being assigned a 'moderate ecological status' and the Solent a subject to eutrophication (Painting et al., 2016). However, it should be noted here that much of the data for the ecological status of the region by the Environmental Agency are now 8 years out of date and could be an underestimation considering that the number of reported sewage spills has more than doubled since 2015 (https://www.gov.uk/government/publications/water-and-sewerage-companies-in-england-environmental-performance-report-2022/southern-water-epa-data-report-2022). In comparison to other UK counties, Hampshire is subjected to fewer such outfalls than other counties, with <8000 incidents in Hampshire in 2021 and 2022 compared to Cornwall (> 25,000) or Devon (>50,000) (Fig. 1). It is therefore likely that coastal settings, including those under RAMSAR or SSSI status in other counties and countries with temperate coastlines experience increased anthropogenic

nutrient input from stormwater and sewage spills, causing intensified eutrophication, hypoxia and associated increased risk of macroalgal settling and harmful algal blooms (Boyes and Elliott, 2006; Menesguen et al., 2014). In fact, coastal settings throughout the Solent and English Channel, including Langstone Harbour, have seen a surge in occurrence of *Ulva* spp. beds contributing to poor ecological status of the coastal ocean (Tappin and Millward, 2015).

4.2. Seasonal-driven differences in environmental conditions

Water temperatures ranged between 8.5 and 9.2 °C in winter and 17.4–20.2 °C in summer, representative for the Solent and English Channel (Table 1). However, 20.2 °C recorded in July and August 2021 was above typical average temperatures of 18 °C, indicating a period of localised warming which could be classified as a short-term marine heatwave (Widdicombe et al., 2010; Hobday et al., 2016). There was strong seasonality in environmental conditions, whereby increased temperatures and associated increased light, rather than nutrient availability led to the succession of the microbial community observed in summer (Smyth et al., 2010) (Fig. 4). The observed reduction in dissolved nutrient concentrations in spring coincided with the increase in planktonic abundance, suggesting that consumption of the dissolved nutrients led to diminished availability of inorganic nutrients over the summer months (0.89 ± 0.56 μmol NO_3^- L^{-1} and 0.09 ± 0.03 μmol PO_4^{3-} L^{-1}), whereby a N:P ratio (10 ± 3) establishes the study site as a predominantly N-limited system (Fig. 2). Further, increased freshwater input of nutrients into the system or consumption by macrofauna could possibly contribute to decreased nutrient concentrations at the monitoring site, which however seem unlikely due to clearly marine water body. Despite a N-limited water column, enhanced planktonic abundance and biomass was observed during summer, and blooms occurred both in spring and autumn as evident from the distinct peaks in Chl *a* observed in March, May and August (Fig. 3). The larger abundance of planktonic organisms appeared to be the main driver for the decrease in inorganic nutrient concentrations during spring, increased production and recycling of organic matter at the offset of the blooming event could maintain phytoplankton abundance and biomass throughout the summer. Moreover, enhanced planktonic activity also produces DOP (Reynolds et al., 2014), here suggested by the correlation with DOP, that could further support primary production over the nutrient limited summer months, as DOP is remineralised by heterotrophic bacteria, or possibly directly accessed by phytoplankton (Dyhrman and Ruttenberg, 2006; Diaz et al., 2018; Breton et al., 2022). Increases in inorganic nutrients were observed between September and October and are likely the result of the breakdown of density stratification, mixing NO_3^- into surface waters, and enhanced nitrification activity following the breakdown of late summer phytoplankton blooms (Smyth et al., 2010).

4.3. Seasonality in microbial community structure

At the monitoring station, water temperature and increased light availability are likely responsible for shaping the planktonic community on a seasonal scale (Trombetta et al., 2019, 2021). A similar trend in phytoplankton abundance and community structure has previously been observed at the Western Channel Observatory (WCO), Plymouth, UK (Widdicombe et al., 2010). Moreover, additional data on larger phytoplankton groups at WCO shows that diatoms display maximum growth rates, specifically under elevated nutrient availability, and thus are mainly associated with the spring bloom (Widdicombe et al., 2010). Although microalgal abundances were not determined in this study, this pattern could be inferred from the observed reduction in DSi during March (−77 %, ΔDSi 5.27 ± 2.54 μmol L^{-1}) (Fig. 2), indicating that diatom species were likely major contributors to the observed peak in Chl *a* biomass. Likewise, the observed blooming event in late summer coincided with a sudden decrease in DSi in August(− 19 %, ΔDSi 0.93 ± 0.18 μmol L^{-1}) (Fig. 2), thus suggesting diatoms contribute substantially to primary production in the Solent (Breton et al., 2022; Wei et al., 2022). This is further supported by the weak correlation of *Synechococcus* and Chl *a* observed, whereas eukaryotic organisms had a higher relative contribution towards Chl *a*. This is in line with observations in the western English Channel, where the autumn bloom was associated with diatoms (Widdicombe et al., 2010).

Zooplankton grazing exerts an important top-down control on phytoplankton biomass, specifically in highly productive coastal settings (Widdicombe et al., 2010; Bresnan et al., 2015; Chen et al., 2016). Zooplankton grazers are found increasingly abundant between March and August, following planktonic blooming events (Bresnan et al., 2015). It is highly likely that the peaks in pheophytin *a* observed during summer were associated with increased grazing pressure as a consequence of higher food availability, rather than increased planktonic mortality alone (Chen et al., 2016). Although *Synechococcus* and nanoeukaryotes correlated strongly with pheophytin *a*, peaks in pheophytin *a* were more likely the result of the dying off of larger cells following the breakdown of the blooming events (Fig. 3). Moreover, the warming event observed in July and August 2021 contributed to high pheophytin *a* concentrations, likely due to cell senescence and mortality, increasing the grazing pressure further (Chen et al., 2016). During this period, pheophytin *a* peaked (3.6 μg L^{-1}), whilst Chl *a* decreased to the lowest concentration (0.6 μg L^{-1}) observed throughout the year-long monitoring (Fig. 3). Simultaneously, *Synechococcus* decreased (−42 %) and nanoeukaryotes decreased (−26 %) in abundance between July and August, suggesting increased grazing pressure following the breakdown of the spring bloom, in conjunction with higher mortality.

4.4. Seasonal organic matter dynamics

The community structure of primary producers and their productivity sets the control on organic matter and carbon fixation on an annual scale throughout the Solent and English Channel (Litt et al., 2010; Martinez-Vicente et al., 2010). However, the pico- and nanoeukaryotic primary producers determined at our monitoring station did not seem to explain seasonal variability in POM. Instead, correlation with algal and bacterial cells suggest that organic material derived from larger planktonic organisms or macrophytes and its bacterial degradation drives POM dynamics, which has also been suggested at the WCO (Martinez-Vicente et al., 2010). Indeed, higher POM concentrations were found in spring and summer due to enhanced planktonic abundance and productivity, and subsequent remineralisation processes. The POM pool generally contains higher amounts of phytoplankton derived organic matter during the more productive spring and summer season, whilst organic detritus comprises the majority in autumn and winter (Martinez-Vicente et al., 2010). There was low seasonal variability in POM observed at our monitoring site, and the POM versus Chl *a* regression suggested that the majority of POM, at least POC and PP, was produced autochthonously (Fig. 5). However, heterotrophic activity could greatly influence POM formation and Litt et al. (2010) associated enhanced bacterial activity to the offset of blooming events and the subsequent breakdown of accumulated organic matter. In fact, dissolved oxygen was lowest (6.7–7.6 mg L^{-1}) between June and October, suggesting increased heterotrophic activity, alongside higher water temperatures, which also contributed to lower oxygen concentrations. Heterotrophic bacterial abundance was higher in summer (up to 1.2×10^6 cell counts mL^{-1}) and decreased substantially in winter (below 0.3×10^6 cell counts mL^{-1}). Increased biological oxygen consumption would suggest enhanced respiration within the system, exceeding photosynthetic activity (Martinez-Vicente et al., 2010). Whilst these explanations hold for POC and PP, the majority of PON was found to be of allochthonous origin. Highest PON concentrations were measured in spring and autumn, corresponding to enhanced phytoplanktonic abundance and biomass following blooming events, whilst PON was lowest in summer, during which phytoplanktonic abundance was highest. Wyatt et al. (2010) associated intensifying drawdown of atmospheric ammonia

(NH_3) to elevated surface ammonium (NH_4^+) concentrations, a preferred nitrogen source to marine microbes, which is specifically important during the N-limited conditions during summer. Atmospheric deposition of nitrogen can thus be considered an allochthonous source of N (Wyatt et al., 2010). This is likely the case at our monitoring site in summer, during which the dissolved organic fraction of nutrients dominated the total pool of available nutrients (Fig. 2). Elevated signals of PON in spring and autumn could further be associated to increased inflow of N from external sources, such as riverine and urban runoff, tidal flushing or macroalgal fragmentation carrying organic material (Dailer et al., 2010; Naden et al., 2016). Given that our monitoring station is clearly a marine water body, it can also be inferred that more frequent precipitation and associated stormwater and sewage releases are most likely sources of increased N loading to the Solent (Naden et al., 2016).

5. Conclusion and broader perspective

This study revealed a substantial amount of excess nutrient input into the Solent, contributing to its poor ecological status. However, the phytoplanktonic community, crucial for assessing ecological health in coastal areas, and biogeochemical functioning did show acclimation to nutrient pollution and resilience to the periodic excess input. Seasonal variations in environmental conditions, mainly temperature and light availability, rather than nutrient availability, drove phytoplankton abundance and biomass and associated organic matter dynamics. Despite adaptation to sub-annual environmental fluctuations, influxes of excess nutrients from stormwater and sewage overflows raise concerns about coastal eutrophication and impacts on the planktonic community, and subsequently, impacts on ecosystem functioning and biogeochemical cycling in the coastal ocean. These monitoring efforts in the Solent provide valuable insights applicable to similar coastal settings, emphasizing the need for long-term monitoring to better understand ecosystem changes and to inform management and protection plans, especially in light of increasing anthropogenic disturbances and progressing climate change. A network of monitoring stations such as Langstone Harbour, focusing on small planktonic communities and the cycling of nutrients and carbon, is needed for other coastal areas on the Southcoast of the UK, to reflect location-specific hydrographical features and to support effective management efforts.

CRediT authorship contribution statement

Lukas Marx: Writing – review & editing, Writing – original draft, Visualization, Validation, Methodology, Investigation, Formal analysis, Data curation, Conceptualization. **Michelle Hale:** Writing – review & editing, Resources, Project administration, Funding acquisition. **B.B. Cael:** Writing – review & editing, Methodology, Formal analysis, Data curation. **Sarah Reynolds:** Writing – review & editing, Methodology, Funding acquisition, Formal analysis, Data curation, Conceptualization.

Funding

This work was supported by the University of Portsmouth Faculty of Science and Health PhD bursary scheme.

Declaration of competing interest

The authors declare that the research was conducted in the absence of any commercial or financial relationships that could be construed as a potential conflict of interest.

Acknowledgements

The authors thank the Institute of Marine Sciences (IMS) Portsmouth for access and resources.

Appendix A. Supplementary data

Supplementary data to this article can be found online at https://doi.org/10.1016/j.marpolbul.2025.117982.

Data availability

The data for this research is made available in the supplementary data.

References

Bell, V.A., Naden, P.S., Tipping, E., Davies, H.N., Carnell, E., Davies, J.A.C., Wu, L., 2021. Long term simulations of macronutrients (C, N and P) in UK freshwaters. Sci. Total Environ. 776, 145813.

Boyes, S., Elliott, M., 2006. Organic matter and nutrient inputs to the Humber estuary. England. Marine pollution bulletin 53 (1–4), 136–143.

Bresnan, E., Cook, K.B., Hughes, S.L., Hay, S.J., Smith, K., Walsham, P., Webster, L., 2015. Seasonality of the plankton community at an east and west coast monitoring site in Scottish waters. J. Sea Res. 105, 16–29. https://doi.org/10.1016/j.seares.2015.06.009.

Breton, E., Goberville, E., Sautour, B., Ouadi, A., Skouroliakou, D.I., Seuront, L., Beaugrand, G., Kléparski, L., Crouvoisier, M., Pecqueur, D., Salmeron, C., Cauvin, A., Poquet, A., Garcia, N., Gohin, F., Christaki, U., 2022. Multiple phytoplankton community responses to environmental change in a temperate coastal system: A trait-based approach. Front. Mar. Sci. 9. https://doi.org/10.3389/fmars.2022.914475.

Chen, J., Oseji, O., Mitra, M., Waguespack, Y., Chen, N., 2016. Phytoplankton pigments in Maryland Coastal Bay sediments as biomarkers of sources of organic matter to benthic community. J. Coast. Res. 32 (4), 768–775. https://doi.org/10.2112/JCOASTRES-D-14-00223.1.

Dailer, M.L., Knox, R.S., Smith, J.E., Napier, M., Smith, C.M., 2010. Using δ15N values in algal tissue to map locations and potential sources of anthropogenic nutrient inputs on the island of Maui, Hawai ‘i, USA. Mar. Pollut. Bull. 60 (5), 655–671.

Davis, C.E., Mahaffey, C., Wolff, G.A., Sharples, J., 2014. A storm in a shelf sea: Variation in phosphorus distribution and organic matter stoichiometry. Geophys. Res. Lett. 41 (23), 8452–8459. https://doi.org/10.1002/2014GL061949.

Davis, C.E., Blackbird, S., Wolff, G., Woodward, M., Mahaffey, C., 2019. Seasonal organic matter dynamics in a temperate shelf sea. Prog. Oceanogr. 177. https://doi.org/10.1016/j.pocean.2018.02.021.

Devlin, M.J., Prins, T.C., Enserink, L., Leujak, W., Heyden, B., Axe, P.G., Iglesias-Campos, A., 2023. A first ecological coherent assessment of eutrophication across the north-East Atlantic waters (2015–2020). Frontiers in Ocean Sustainability 1.

Diaz, J.M., Holland, A., Sanders, J.G., Bulski, K., Mollett, D., Chou, C.W., Phillips, D., Tang, Y., Duhamel, S., 2018. Dissolved organic phosphorus utilization by phytoplankton reveals preferential degradation of polyphosphates over phosphomonoesters. Front. Mar. Sci. 5 (OCT). https://doi.org/10.3389/fmars.2018.00380.

Dyhrman, S.T., Ruttenberg, K.C., 2006. Presence and regulation of alkaline phosphatase activity in eukaryotic phytoplankton from the coastal ocean: Implications for dissolved organic phosphorus remineralization. Limnol. Oceanogr. 51 (3), 1381–1390.

Foster, N.M., Hudson, M.D., Bray, S., Nicholls, R.J., 2013. Intertidal mudflat and saltmarsh conservation and sustainable use in the UK: A review. In. J. Environ. Manag. 126, 96–104. https://doi.org/10.1016/j.jenvman.2013.04.015.

Gac, J.P., Marrec, P., Cariou, T., Grosstefan, E., Macé, É., Rimmelin-Maury, P., Vernet, M., Bozec, Y., 2021. Decadal dynamics of the CO2 system and Associated Ocean acidification in coastal ecosystems of the north East Atlantic Ocean. Front. Mar. Sci. 8. https://doi.org/10.3389/fmars.2021.688008.

Hammond, P., Suttie, M., Lewis, V.T., Smith, A.P., Singer, A.C., 2021. Detection of untreated sewage discharges to watercourses using machine learning. NPJ Clean Water 4 (1), 18.

Harris, R., 2010. The L4 time-series: The first 20 years. In. J. Plankton Res. 32 (5), 577–583. https://doi.org/10.1093/plankt/fbq021.

Hauck, J., Zeising, M., Le Quéré, C., Gruber, N., Bakker, D.C., Bopp, L., Séférian, R., 2020. Consistency and challenges in the ocean carbon sink estimate for the global carbon budget. Front. Mar. Sci. 7, 571720.

Helmer, L., Farrell, P., Hendy, I., Harding, S., Robertson, M., Preston, J., 2019. Active management is required to turn the tide for depleted Ostrea edulis stocks from the effects of overfishing, disease and invasive species. PeerJ 2019 (2). https://doi.org/10.7717/peerj.6431.

Hobday, A.J., Alexander, L.V., Perkins, S.E., Smale, D.A., Straub, S.C., Oliver, E.C., Wernberg, T., 2016. A hierarchical approach to defining marine heatwaves. Prog. Oceanogr. 141, 227–238.

IPCC, 2021. In: Masson-Delmoote, V., Zhai, P., Pirani, A., Connors, S.L., Péan, C., Berger, S., et al. (Eds.), Climate Change 2021: The Physical Science Basis. Contribution of Working Group I to the Sixth Assessment Report of the Intergovernmental Panel on Climate Change Summary for Policymakers. Cambridge University Press, Cambridge, New York, NY, pp. 3–32.

Kassem, H., Amos, C.L., Thompson, C.E.L., 2023. Sea surface temperature trends in the coastal zone of southern England. J. Coast. Res. 39 (1), 18–31.

Knap, A.H., Michaels, A., Close, A.R., Ducklow, H., Dickson, A.G., 1996. Protocols for the joint global ocean flux study (JGOFS) core measurements. In: JGOFS, reprint of the IOC manuals and guides no. 29, UNESCO 1994, 19.

Kruskal, W.H., Wallis, W.A., 1952. Use of ranks in one-criterion variance analysis. J. Am. Stat. Assoc. 47 (260), 583–621.

Levasseur, A., 2008. Observations and Modelling of the Variability of the Solent-Southampton Water Estuarine System (Doctoral dissertation, University of Southampton). https://eprints.soton.ac.uk/63761/.

Litt, E.J., Hardman-Mountford, N.J., Blackford, J.C., Mitchelson-Jacob, G., Goodman, A., Moore, G.F., Cummings, D.G., Butenschön, M., 2010. Biological control of pCO2 at station L4 in the Western English Channel over 3 years. J. Plankton Res. 32 (5), 621–629. https://doi.org/10.1093/plankt/fbp133.

Liu, X., Stock, C.A., Dunne, J.P., Lee, M., Shevliakova, E., Malyshev, S., Milly, P.C., 2021. Simulated global coastal ecosystem responses to a half-century increase in river nitrogen loads. Geophys. Res. Lett. 48 (17), e2021GL094367.

Lomas, M.W., Burke, A.L., Lomas, D.A., Bell, D.W., Shen, C., Dyhrman, S.T., Ammerman, J.W., 2010. Sargasso Sea phosphorus biogeochemistry: an important role for dissolved organic phosphorus (DOP). Biogeosciences. www.biogeosciences.net/7/695/2010/.

Lønborg, C., Müller, M., Butler, E.C., Jiang, S., Ooi, S.K., Trinh, D.H., Martin, P., 2021. Nutrient cycling in tropical and temperate coastal waters: is latitude making a difference? Estuar. Coast. Shelf Sci. 262, 107571.

Martinez-Vicente, V., Land, P.E., Tilstone, G.H., Widdicombe, C., Fishwick, J.R., 2010. Particulate scattering and backscattering related to water constituents and seasonal changes in the Western English Channel. J. Plankton Res. 32 (5), 603–619. https://doi.org/10.1093/plankt/fbq013.

McQuatters-Gollop, A., Stern, R.F., Atkinson, A., Best, M., Bresnan, E., Creach, V., Tett, P., 2024. The silent majority: Pico-and nanoplankton as ecosystem health indicators for marine policy. Ecol. Indic. 159, 111650.

Menesguen, A., Dussauze, M., Lecornu, F., Dumas, F., Thouvenin, B., 2014. Operational modelling of nutrients and phytoplancton in the bay of Biscay and english channel. Mercator Ocean-Quarterly Newsletter 49, 87–93.

Moore, C.M., Mills, M.M., Arrigo, K.R., Berman-Frank, I., Bopp, L., Boyd, P.W., Galbraith, E.D., Geider, R.J., Guieu, C., Jaccard, S.L., Jickells, T.D., La Roche, J., Lenton, T.M., Mahowald, N.M., Marañón, E., Marinov, I., Moore, J.K., Nakatsuka, T., Oschlies, A., Ulloa, O., 2013. Processes and patterns of oceanic nutrient limitation. In Nature Geoscience 6 (Issue 9), 701–710. https://doi.org/10.1038/ngeo1765.

Naden, P., Bell, V., Carnell, E., Tomlinson, S., Dragosits, U., Chaplow, J., May, L., Tipping, E., 2016. Nutrient fluxes from domestic wastewater: A national-scale historical perspective for the UK 1800–2010. Sci. Total Environ. 572, 1471–1484. https://doi.org/10.1016/j.scitotenv.2016.02.037.

Painting, S., Garcia, L., Collingridge, K., 2016. Common Procedure for the Identification of the Eutrophication Status of the UK Maritime Area. UK National Report.

Pontee, N., 2013. Defining coastal squeeze: A discussion. In: Ocean and Coastal Management, vol. 84. Elsevier Ltd., pp. 204–207. https://doi.org/10.1016/j.ocecoaman.2013.07.010

R Core Team, . R: A language and environment for statistical computing. *https://www.R-project.org/*. In: R Foundation for Statistical Computing. Vienna, Austria.

Reynolds, S., Mahaffey, C., Roussenov, V., Williams, R.G., 2014. Evidence for production and lateral transport of dissolved organic phosphorus in the eastern subtropical North Atlantic. Glob. Biogeochem. Cycles 28 (8), 805–824.

Roobaert, A., Laruelle, G.G., Landschützer, P., Gruber, N., Chou, L., Regnier, P., 2019. The spatiotemporal dynamics of the sources and sinks of CO2 in the global coastal ocean. Glob. Biogeochem. Cycles 33 (12), 1693–1714.

Rühl, S., Thompson, C.E., Queirós, A.M., Widdicombe, S., 2020. Intra-annual patterns in the benthic-pelagic fluxes of dissolved and particulate matter. Front. Mar. Sci. 7, 567193.

Santos, I.R., Chen, X., Lecher, A.L., Sawyer, A.H., Moosdorf, N., Rodellas, V., Li, L., 2021. Submarine groundwater discharge impacts on coastal nutrient biogeochemistry. Nature Reviews Earth & Environment 2 (5), 307–323.

Shapiro, S.S., Wilk, M.B., 1965. An analysis of variance test for normality (complete samples). Biometrika 52 (3/4), 591–611.

Smyth, T.J., Fishwick, J.R., Al-Moosawi, L., Cummings, D.G., Harris, C., Kitidis, V., Rees, A., Martinez-Vicente, V., Woodward, E.M.S., 2010. A broad spatio-temporal view of the Western English Channel observatory. J. Plankton Res. 32 (5), 585–601. https://doi.org/10.1093/plankt/fbp128.

Tappin, A.D., Millward, G.E., 2015. The English Channel: Contamination status of its transitional and coastal waters. Mar. Pollut. Bull. 95 (2), 529–550.

Tarran, G.A., Bruun, J.T., 2015. Nanoplankton and picoplankton in the Western English Channel: Abundance and seasonality from 2007–2013. Prog. Oceanogr. 137, 446–455.

Trombetta, T., Vidussi, F., Mas, S., Parin, D., Simier, M., Mostajir, B., 2019. Water temperature drives phytoplankton blooms in coastal waters. PLoS One 14 (4). https://doi.org/10.1371/journal.pone.0214933.

Trombetta, T., Vidussi, F., Roques, C., Mas, S., Scotti, M., Mostajir, B., 2021. Co-occurrence networks reveal the central role of temperature in structuring the plankton community of the Thau lagoon. Sci. Rep. 11 (1), 17675.

Watson, S.C.L., Preston, J., Beaumont, N.J., Watson, G.J., 2020. Assessing the natural capital value of water quality and climate regulation in temperate marine systems using a EUNIS biotope classification approach. Sci. Total Environ. 744. https://doi.org/10.1016/j.scitotenv.2020.140688.

Wei, Y., Ding, D., Gu, T., Jiang, T., Qu, K., Sun, J., Cui, Z., 2022. Different responses of phytoplankton and zooplankton communities to current changing coastal environments. Environ. Res. 215. https://doi.org/10.1016/j.envres.2022.114426.

Widdicombe, C.E., Eloire, D., Harbour, D., Harris, R.P., Somerfield, P.J., 2010. Long-term phytoplankton community dynamics in the Western English Channel. J. Plankton Res. 32 (5), 643–655. https://doi.org/10.1093/plankt/fbp127.

Wyatt, N.J., Kitidis, V., Woodward, E.M.S., Rees, A.P., Widdicombe, S., Lohan, M., 2010. Effects of high CO2 on the fixed nitrogen inventory of the Western English Channel. J. Plankton Res. 32 (5), 631–641. https://doi.org/10.1093/plankt/fbp140.

Yamamuro, M., Kayanne, H., 1995. Rapid direct determination of organic carbon and nitrogen in carbonate-bearing sediments with a Yanaco MT-5 CHN analyzer. Limnol. Oceanogr. 40 (5), 1001–1005.